

# Baryonic $B$ Meson Decays

M.Z. Wang<sup>a\*</sup>

<sup>a</sup>Department of Physics, National Taiwan University,  
Taipei, Taiwan, R.O.C.

Recent results of the baryonic  $B$  decays from the two b-factories, BABAR and Belle, are presented. These include studies of charmonium decays from  $B^+ \rightarrow p\bar{p}K^+$  and  $B^+ \rightarrow \Lambda\bar{\Lambda}K^+$ ; observations of  $B^+ \rightarrow J/\psi\bar{\Lambda}p$ ,  $B \rightarrow \Lambda_c^+\bar{\Lambda}_c^-K$ , and  $B^+ \rightarrow \Xi_c^0\Lambda_c^+$  and study of inclusive  $B$  decays to  $\Lambda_c$ .

PACS: 13.25.Hw, 13.60.Rj, 13.40.Hq, 14.20.Lq, 14.20.Dh, 14.40.Nd, 12.15.Hh

## 1. Introduction

The weak decays of  $B$  mesons offer not only the important study of CP violation but also a profound searching ground for the final states containing a baryon-antibaryon pair because of the large mass of  $B$  mesons. Following the pioneering work done by CLEO [1], many exclusive baryonic  $B$  meson decays have been found recently by the two b-factories, BABAR [2] and Belle [3].

In b-factory, it is an over-constrained system to determine decays from  $B$  meson since not only the mass but also the energy of the  $B$  meson are known in the center-of-mass (CM) frame. One can use two kinematic variables in the CM frame to identify the reconstructed  $B$  meson candidates: the beam energy constrained mass  $M_{bc} = \sqrt{E_{\text{beam}}^2 - p_B^2}$ , and the energy difference  $\Delta E = E_B - E_{\text{beam}}$ , where  $E_{\text{beam}}$  is the beam energy, and  $p_B$  and  $E_B$  are the momentum and energy, respectively, of the reconstructed  $B$  meson. Alternatively, one can use  $M_{bc}$  and  $\Delta M_B$ , where  $\Delta M_B$  is the mass difference between the reconstructed  $B$  mass and the nominal  $B$  mass [4]. To determine the  $B$  yields, normally an unbinned extended likelihood fit is applied by using the above two variables as inputs for all candidate events. The signal probability density function (PDF) of the two variables is typically obtained by Monte Carlo samples and the background PDF is determined from sideband (i.e. non-signal region) data.

## 2. Charmless modes

After the first observation of the charmless baryonic  $B$  meson decay,  $B^+ \rightarrow p\bar{p}K^+$  [5,6], many charmless three-body baryonic decays are found [7]. The dominant contributions for these decays are presumably via the  $b \rightarrow s$  penguin diagram except that for  $B^+ \rightarrow p\bar{p}\pi^+$  which is believed to be the  $b \rightarrow u$  tree diagram. There is a common feature of these decays that the dibaryon mass spectra show an enhancement near threshold. This feature was conjectured in Refs. [8] and aroused more theoretical interests lately. Detailed information from the polar angle distributions [9] and Dalitz plot [10] offer better understanding of the underlying dynamics.

Fig. 1 shows the recent results [11] from  $B^+ \rightarrow p\bar{p}K^+$  and  $B^+ \rightarrow \Lambda\bar{\Lambda}K^+$  obtained by Belle with  $386 \times 10^6 B\bar{B}$  pairs. There are clear threshold enhancement,  $\eta_c$  and  $J/\psi$  peaks in the baryon-antibaryon mass spectrum. A maximum likelihood fit to the data is shown in the inset, with a relativistic Breit-Wigner function for the  $\eta_c$  peak, a Gaussian for the  $J/\psi$  peak, and a linear function for the non-resonant background. The Breit-Wigner function is convolved with the detector response function, which is taken from the  $J/\psi$  peak. One then obtains an  $\eta_c$  mass of  $M_{\eta_c} = 2971 \pm 3_{-1}^{+2}$  MeV/ $c^2$  ( $2974 \pm 7_{-1}^{+2}$  MeV/ $c^2$ ) and a width of  $\Gamma(\eta_c) = 48_{-7}^{+8} \pm 5$  MeV/ $c^2$  ( $40 \pm 19 \pm 5$  MeV/ $c^2$ ) for the  $\eta_c \rightarrow p\bar{p}$  ( $\eta_c \rightarrow \Lambda\bar{\Lambda}$ ) mode. The width is larger than the PDG average but is consistent with recent BABAR [10] and previous Belle [12] measurements. This is also the first ob-

\*on behalf of the Belle Collaboration

servation of  $\eta_c \rightarrow \Lambda \bar{\Lambda}$  decays with  $\mathcal{B}(\eta_c \rightarrow \Lambda \bar{\Lambda}) = (0.87_{-0.21}^{+0.24}(\text{stat})_{-0.14}^{+0.09}(\text{syst}) \pm 0.27(\text{PDG})) \times 10^{-3}$ .

From this data set, one can also determine the branching fraction ratios:  $\mathcal{B}(\eta_c \rightarrow \Lambda \bar{\Lambda})/\mathcal{B}(\eta_c \rightarrow p \bar{p}) = 0.67_{-0.16}^{+0.19} \pm 0.12$  and  $\mathcal{B}(J/\psi \rightarrow \Lambda \bar{\Lambda})/\mathcal{B}(J/\psi \rightarrow p \bar{p}) = 0.90_{-0.14}^{+0.15} \pm 0.10$ , where common systematic errors in the numerator and denominator cancel. The observed ratio is consistent with theoretical expectation [13] based on a quark-diquark model for baryons.

### 3. Charmed Modes

The  $b \rightarrow c$  process is the dominant process for  $B$  decays. Many decay modes with  $\Lambda_c^+$  in the final states have been found, including the first observation of a two-body decay:  $B^0 \rightarrow p \bar{\Lambda}_c^-$  [14]. It is interesting to see that the two-body baryonic decay is suppressed in exclusive  $B$  decays. Comparing with mesonic  $B$  decays, two-body and three-body decays are comparable. This indicates that for the formation of a baryon-antibaryon pair, giving off extra energy is much favored.

The excess in the low momentum region of the inclusive  $J/\psi$  spectrum for  $B$  decays is not consistent with predictions from non-relativistic QCD calculations. With the hint of threshold enhancement, this triggers the search for decay modes like  $B^+ \rightarrow J/\psi \bar{\Lambda} p$ . Evidence is reported by BABAR [15] with  $8.9 \times 10^6 B \bar{B}$  pairs. Using larger data set,  $275 \times 10^6 B \bar{B}$  pairs, Belle has made the observation [16] and obtained a branching fraction of  $\mathcal{B}(B^+ \rightarrow J/\psi \bar{\Lambda} p) = (11.6 \pm 2.8_{-2.3}^{+1.8}) \times 10^{-6}$ . This is not large enough to explain the observed excess. However, it stimulates more efforts to search for similar modes. Fig. 2 shows the  $M_{bc} - \Delta M_B$  scatter plots and their projections for candidate events.

Similar decay process via the  $b \rightarrow c \bar{c} s$  transition and limited phase space has been found for  $B^+ \rightarrow \Lambda_c^+ \bar{\Lambda}_c^- K^+$  and  $B^0 \rightarrow \Lambda_c^+ \bar{\Lambda}_c^- K^0$  [17] with a  $386 \times 10^6 B \bar{B}$  data sample. The measured branching fractions are unexpectedly large:  $\mathcal{B}(B^+ \rightarrow \Lambda_c^+ \bar{\Lambda}_c^- K^+) = (6.5_{-0.9}^{+1.0} \pm 1.1 \pm 3.4) \times 10^{-4}$  and  $\mathcal{B}(B^0 \rightarrow \Lambda_c^+ \bar{\Lambda}_c^- K^0) = (7.9_{-2.3}^{+2.9} \pm 1.2 \pm 4.1) \times 10^{-4}$ . Again this large rate can be understood by the threshold enhancement phenomenon. Observation of this kind of decay is important for the

determination of the charm particle yield per  $B$  decay. Decays like  $B \rightarrow \Lambda_c^+ \bar{\Lambda}_c^- K$  would give a wrong-sign  $\Lambda_c^+$ , where for most cases only  $\bar{\Lambda}_c^-$ 's are present in the final state from  $B$  decays.

Along the doubly charmed baryon track, another two-body decay has been found in the same data set. Its decay diagram is shown in Fig. 3 which is quite similar to that of  $B^0 \rightarrow \bar{\Lambda}_c^- p$ . One only needs to replace the  $c \bar{s}$  with  $u \bar{d}$  and  $d \bar{d}$  with  $u \bar{u}$  to make the change. Therefore, one would expect these two decay modes have similar branching fractions. However, the measured branching fraction product [18]  $\mathcal{B}(B^+ \rightarrow \Xi_c^0 \Lambda_c^+) \times \mathcal{B}(\Xi_c^0 \rightarrow \Xi^+ \pi^-) = (4.8_{-0.9}^{+1.0} \pm 1.1 \pm 1.2) \times 10^{-4}$  is too big. Assuming  $\mathcal{B}(\Xi_c^0 \rightarrow \Xi^+ \pi^-)$  is at 1% level, then  $\mathcal{B}(B^+ \rightarrow \Xi_c^0 \Lambda_c^+) \sim 10^{-3}$ . This is about 100 times bigger than that of  $B^0 \rightarrow \bar{\Lambda}_c^- p$ . This is another example of enhancement for smaller available energy in the baryon-antibaryon system. Fig. 4 shows the observed signals and hints for background with similar final state particles.

The charm counting problem of  $B$  decays is a fundamental issue to be solved. Using fully reconstructed  $B$  sample (flavor tagging), one can study the correlated ( $b \rightarrow c$ ) and anti-correlated ( $b \rightarrow \bar{c}$ ) charm production from other  $B$  decays. Presumably the correlated charm production is dominant and the anti-correlated is suppressed with a phase space factor. Experimentally, one can determine the correlated/anti-correlated charm production by studying the inclusive  $B$  decay rates to a limited charm hadrons, e.g.  $\Lambda_c^+$ , because all other heavier charm particles decay into one of these special cases. Recently, BABAR used a  $231 \times 10^6 B \bar{B}$  sample and made the measurement [19]. The charm yield per  $B$  decay is around 1.2.

### 4. Summary

The exclusive baryonic  $B$  decays are well established after a few year's running of the two factories. It seems that to understand the threshold enhancement is a key for constructing the proper decay mechanism. The study of baryonic  $B$  decays is booming with fast accumulated data samples. Many unexpected things like rare decays from both charm and beauty mesons, and

even exotic states (e.g. pentaquark) could be the by-products.

## REFERENCES

1. X. Fu *et al.* (CLEO Collaboration), Phys. Rev. Lett. **79**, 3125 (1997).
2. B. Aubert *et al.* (BABAR Collaboration), Nucl. Instr. and Meth. A **479**, 1 (2002).
3. A. Abashian *et al.* (Belle Collaboration), Nucl. Instr. and Meth. A **479**, 117 (2002).
4. S. Eidelman *et al.* (Particle Data Group), Phys. Lett. B **592**, 594 (2004).
5. K. Abe *et al.* (Belle Collaboration), Phys. Rev. Lett. **88**, 181803 (2002).
6. Throughout this report, inclusion of charge conjugate mode is always implied unless otherwise stated.
7. M.Z. Wang *et al.* (Belle Collaboration), Phys. Rev. Lett. **92**, 131801 (2004).
8. W.S. Hou and A. Soni, Phys. Rev. Lett. **86**, 4247 (2001).
9. M.Z. Wang *et al.* (Belle Collaboration), Phys. Lett. B **617**, 141 (2005).
10. B. Aubert *et al.* (BABAR Collaboration), Phys. Rev. D **72**, 051101 (2005).
11. C.H. Wu *et al.* (Belle Collaboration), hep-ex/0606022.
12. F. Fang *et al.* (Belle Collaboration), Phys. Rev. Lett. **90**, 071801 (2003).
13. M. Anselmino, F. Caruso, S. Forte and B. Pire, Phys. Rev. D **38**, 3516 (1988).
14. N. Gabyshev *et al.* (Belle Collaboration), Phys. Rev. Lett. **90**, 141802 (2003).
15. B. Aubert *et al.* (BABAR Collaboration), Phys. Rev. Lett. **90**, 231 (2003).
16. Q.L. Xie *et al.* (Belle Collaboration), Phys. Rev. D **72**, 051105 (2005).
17. N. Gabyshev *et al.* (Belle Collaboration), hep-ex/0508015.
18. R. Chistov *et al.* (Belle Collaboration), hep-ex/0510074.
19. B. Aubert *et al.* (BABAR Collaboration), hep-ex/0606026.

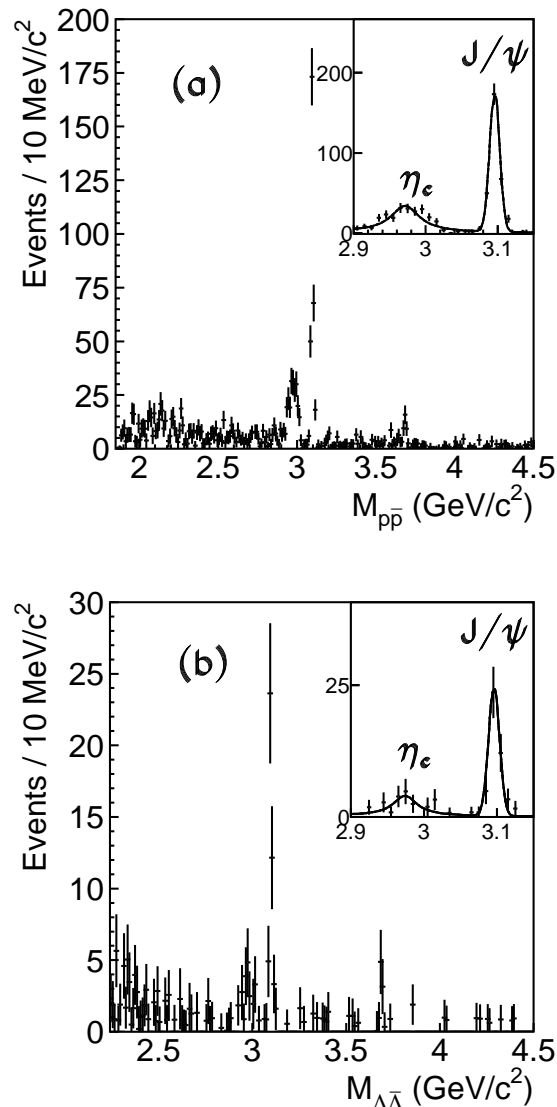


Figure 1. (a)  $B$  signal yield versus  $M_{p\bar{p}}$  and (b)  $B$  signal yield versus  $M_{\Lambda\bar{\Lambda}}$ . The inset shows the  $\eta_c$ - $J/\psi$  mass region. The curves represent the unbinned likelihood fits to the data.

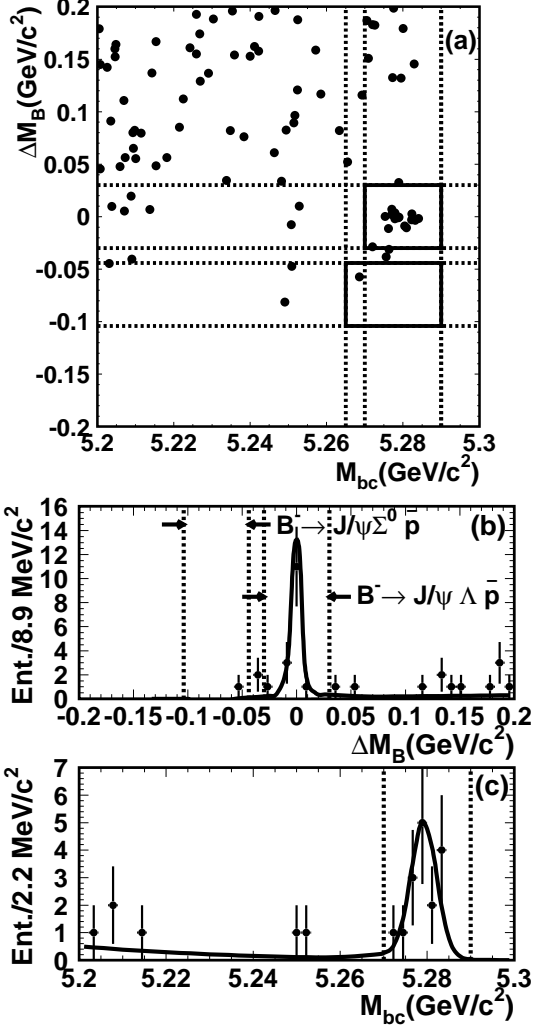


Figure 2. (a) The  $(M_{bc}, \Delta M_B)$  scatter plot of  $B^+ \rightarrow J/\psi \Lambda p$  candidates and its projection onto (b)  $\Delta M_B$  with  $5.265 \text{ GeV}/c^2 < M_{bc} < 5.29 \text{ GeV}/c^2$  and (c)  $M_{bc}$  with  $|\Delta M_B| < 0.03 \text{ GeV}/c^2$ . The dashed lines and solid boxes indicate the signal regions. The curves are the results of the fit.

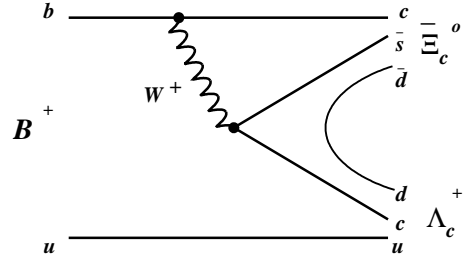


Figure 3. The quark diagram for the  $B^+ \rightarrow \Xi_c^0 \Lambda_c^+$  decay.

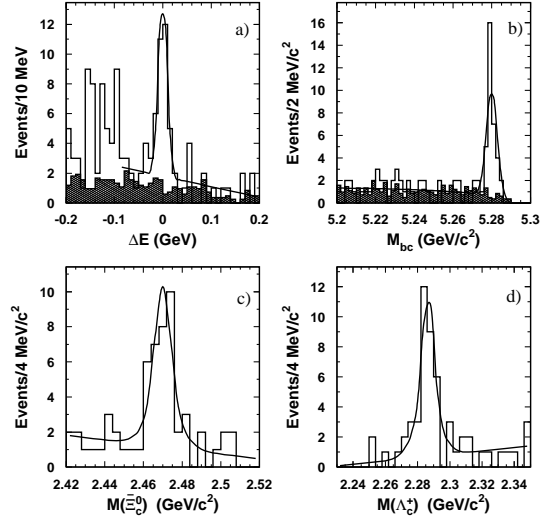


Figure 4. The (a)  $\Delta E$  and (b)  $M_{bc}$  distributions for the  $B^+ \rightarrow \Xi_c^0 \Lambda_c^+$  candidates. The hatched histograms show the combined  $\Xi_c^0$  and  $\Lambda_c^+$  mass sidebands normalized to the signal region. The excess around low  $\Delta E$  region may be due to decays with extra final state particle, e.g.  $\Xi_c^0 \Lambda_c^+ \pi^0$ . The (c)  $\Xi_c^0$  and (d)  $\Lambda_c^+$  mass distributions for candidates taken from the  $B$ -signal region. The overlaid curves are the fit results.